Articles

High-Spin and Spin-Crossover Behavior in Monomethylated Bis(indenyl)chromium(II) Complexes

M. Brett Meredith,[†] Jeffrey A. Crisp,[†] Erik D. Brady,[†] Timothy P. Hanusa,*[,†] Gordon T. Yee,*[,‡] Neil R. Brooks,[§] Benjamin E. Kucera,[§] and Victor G. Young, Jr.[§]

Department of Chemistry, Vanderbilt University, Nashville, Tennessee 37235, Department of Chemistry, Virginia Polytechnic Institute and State University, Blacksburg, Virginia 24061, and X-ray Crystallographic Laboratory, Chemistry Department, University of Minnesota, Minneapolis, Minnesota 55455

Received June 19, 2006

Previous work on bis(indenyl)chromium(II) complexes substituted with bulky groups (*i*-Pr, *t*-Bu, $SiMe_3$) found that their spin state ($S = 1$ or 2) depended on the symmetry of the molecules. Complexes with inversion symmetry (staggered rings) were high-spin; lower symmetry compounds with twisted (gauche) ligands were low spin. The present work explores the effect of methyl group substitution on the indenyl ligand, which leads to complexes possessing either staggered or eclipsed conformations. The monosubstituted compounds [(1 or 2)-$MeC_9H_6]_2Cr$ are prepared from the substituted alkali metal indenides and $CrCl_2$ in THF. X-ray diffraction results indicate that (2-$MeC_9H_6)_2Cr$ exists in a staggered conformation, with Cr−C (av) = 2.308(7) Å, and is a high-spin species in the solid state and solution. In contrast, the monomeric (1-$MeC_9H_6)_2Cr$ is eclipsed in the solid state, where it exhibits spin-crossover behavior over a wide temperature range; the average Cr−C distances vary with temperature, from 2.179(9) Å at 105 K to 2.262(10) Å at 298 K. An attempt to form (4-$MeC_9H_6)_2Cr$ produced the dimeric, thermally unstable complex (η^5-indenyl′)$_2$(μ,η^3-indenyl′)Cr_2(μ-Cl) instead. Correlations between the structure and magnetic properties in bis(indenyl)chromium(II) complexes have been made with density functional theory calculations, which indicate that an eclipsed ligand conformation supports a high spin state, but not to the extent that the staggered form does.

Introduction

Control of the magnetic properties of metal complexes is considered one of the great challenges in contemporary inorganic chemistry.[1] In pursuit of this goal, which will ultimately affect the use of such compounds in magnetic materials[2] and data storage[3] applications, rational ligand design plays a central role. Metallocene-based complexes have been extensively investigated for these purposes, and variations in the metals, their oxidation states, and ring substituents have led to a variety of species displaying spin-crossover behavior,[4] molecular ferromagnetism,[5] and ferromagnetic/antiferromagnetic exchange.[6] Techniques to manipulate the magnetic ground state of transition-metal-based metallocenes have used ligand substituents that affect the bonding of the ligand to the metal, through either ligand donation[7] or, less commonly, steric forces.[8,9]

Although not important in metallocenes, the *rotational* orientation of the ligands in analogous bis(indenyl)metal complexes can influence the spin state of the molecules.[10] Such control has been demonstrated in ring-substituted bis(indenyl)-Cr(II) complexes. The parent compound bis(indenyl)chromium-(II) ($[Ind_2Cr]_2$) exists as a diamagnetic dimer.[11] The addition

* Corresponding author. E-mail: t.hanusa@vanderbilt.edu.
[†] Vanderbilt University.
[‡] Virginia Polytechnic Institute and State University.
[§] University of Minnesota.

(1) (a) Gaspar, A. B.; Ksenofontov, V.; Seredyuk, M.; Guetlich, P. *Coord. Chem. Rev.* **2005**, *249*, 2661−2676 (b) Gütlich, P.; Hauser, A.; Spiering, H. *Angew. Chem., Int. Ed. Engl.* **1994**, *33*, 2024−2054.
(2) (a) Marin, P.; Hernando, A. *J. Magn. Magn. Mater.* **2000**, *215*−*216*, 729−734. (b) Darling, S. B.; Bader, S. D. *J. Mater. Chem.* **2005**, *15*, 4189−4195. (c) Reiss, G.; Huetten, A. *Nat. Mater.* **2005**, *4*, 725−726.
(3) Albrecht, M.; Schatz, G. *NanoS* **2005**, 19−23.
(4) (a) Koehler, F. H.; Schlesinger, B. *Inorg. Chem.* **1992**, *31*, 2853−9. (b) Cozak, D.; Gauvin, F.; Demers, J. *Can. J. Chem.* **1986**, *64*, 71−5.
(5) (a) Yee, G. T.; Manriquez, J. M.; Dixon, D. A.; McLean, R. S.; Groski, D. M.; Flippen, R. B.; Narayan, K. S.; Epstein, A. J.; Miller, J. S. *Adv. Mater.* **1991**, 3, 309−311. (b) Miller, J. S.; Vazquez, C.; McLean, R. S.; Reiff, W. M.; Aumueller, A.; Huenig, S. *Adv. Mater.* (Weinheim, Ger.) **1993**, *5*, 448−50. (c) O'Hare, D.; Brookes, J.; Watkin, D. J. *J. Mater. Chem.* **1991**, *1*, 691−697. (d) Yee, G. T.; Whitton, M. J.; Sommer, R. D.; Frommen, C. M.; Reiff, W. M. *Inorg. Chem.* **2000**, *39*, 1874−1877. (e) Kaul, B. B.; Durfee, W. S.; Yee, G. T. *J. Am. Chem. Soc.* **1999**, *121*, 6862−6866.
(6) (a) Hilbig, H.; Hudeczek, P.; Koehler, F. H.; Xie, X. (b) Bergerat, P.; Kahn, O. *Inorg. Chem.* **1998**, *37*, 4246−4257.
(7) Freyberg, D. P.; Robbins, J. L.; Raymond, K. N.; Smart, J. C. *J. Am. Chem. Soc.* **1979**, *101*, 892−897.
(8) Sitzmann, H.; Schär, M.; Dormann, E.; Keleman, M. Z. *Anorg. Allg. Chem.* **1997**, *623*, 1609−1613.
(9) Hays, M. L.; Burkey, D. J.; Overby, J. S.; Hanusa, T. P.; Yee, G. T.; Sellers, S. P.; Young, V. G., Jr. *Organometallics* **1998**, *17*, 5521−5527.
(10) Brady, E. D.; Overby, J. S.; Meredith, M. B.; Mussman, A. B.; Cohn, M. A.; Hanusa, T. P.; Yee, G. T.; Pink, M. *J. Am. Chem. Soc.* **2002**, *124*, 9556−9566.
(11) Heinemann, O.; Jolly, P. W.; Krüger, C.; Verhovnik, G. P. J. *Organometallics* **1996**, *15*, 5462−5463.

10.1021/om060534u CCC: $33.50
Publication on Web 09/12/2006

of isopropyl groups to the 1- and 3-positions of the parent indenyl ligand leads to the isolation of the purple, high-spin ($S = 2$) monomeric complex $(Ind^{2i})_2Cr$ with a staggered geometry.[12] Under its centrosymmetry, the *ungerade* combinations of the indenyl π orbitals cannot interact with the d orbitals of chromium. However, the use of more sterically demanding substituents (e.g., *t*-Bu, $SiMe_3$) at the 1,3 positions forces the ligands into a ~90° (gauche) relative orientation, producing green, low-spin ($S = 1$) compounds. The reduction of symmetry allows mixing of the indenyl π orbitals with the metal d orbitals, which increases the HOMO−LUMO gap and produces a low-spin configuration.[10]

In principle, any substituent that breaks the centrosymmetry of a bis(indenyl)Cr(II) complex could lead to non-high-spin complexes. On a practical level, variations in the rotational conformation and hence the symmetry and spin state of the molecule could introduce tunable magnetism in systems such as charge-transfer salts.[13] Access to a wider variety of symmetry-changing substituents, including those less sterically demanding than *t*-Bu or $SiMe_3$, would be useful in their design.

We report here that a single methyl group on the five-membered ring of a bis(indenyl′)$_2$Cr complex is enough to disrupt the dimeric form of the unsubstituted compound and that the methyl group's specific location on the ring can strongly affect the geometry of the complex in the solid state. The resulting change of symmetry gives rise to compounds with distinctly different magnetic and structural properties.

Experimental Section

General Considerations. All manipulations were performed with the rigorous exclusion of air and moisture using high-vacuum, Schlenk, or glovebox techniques. Elemental analyses were performed by Desert Analytics, Tucson, AZ. Infrared data were obtained on an ATI Mattson-Genesis FT-IR spectrometer as KBr pellets prepared as previously described.[14] Melting points were determined on a Laboratory Devices Mel-Temp apparatus in sealed capillaries.

Magnetic Measurements. Variable-temperature solution magnetic susceptibility data were obtained on a Bruker DRX-400 spectrometer using the Evans' NMR method.[15] A small sample (3−10 mg) was placed in a 1.0 mL volumetric flask and diluted with toluene-d_8. After complete mixing, approximately 0.5 mL was placed in an NMR tube with a sealed capillary containing a standard solution of toluene-d_8. The calculations needed to determine the number of unpaired electrons based on these data have been described elsewhere.[16]

Solid state magnetic susceptibility data were obtained on a Quantum Designs MPMS SQUID magnetometer in a field of 1000 G. Magnetization as a function of field was also measured to probe for the presence of any ferromagnetic impurities with some compounds; none were noted. To handle the extremely air- and moisture-sensitive compounds, the previously described sample holder was used;[9] the diamagnetic susceptibility of the sample holder was accepted as the average value of the measurements on several identical sample holders. The diamagnetic correction for each complex was estimated from Pascal's constants.

Materials. Nominally anhydrous chromium(II) chloride (Aldrich) was heated under vacuum (150 °C, 10^{-4} Torr) to ensure complete removal of coordinated water. Potassium 1,1,1,3,3,3-hexamethyldisilazide ($K[N(SiMe_3)_2]$) was purchased from Aldrich. *n*-BuLi was purchased from Aldrich as a solution in hexane and was used as received. 4-Methylindanone was purchased from Aldrich and used as received; it was converted into 4-methylindene following the literature procedure.[17] The 4-methylindene was changed into its potassium salt by treatment with $K[N(SiMe_3)_2]$ in toluene. 1-Methylindenide was prepared from lithium indenide and MeI[18] and converted into its lithium salt by treatment with *n*-BuLi in hexanes. 2-Methylindene (Aldrich) was degassed, and its purity verified with ^{1}H NMR prior to use; it was converted into its potassium salt by treatment with $K[N(SiMe_3)_2]$ in toluene. THF, toluene, and hexanes were distilled under nitrogen from potassium benzophenone ketyl.[19] Toluene-d_8 (Aldrich) was vacuum distilled from Na/K (22/78) alloy and stored over 4A molecular sieves prior to use.

Synthesis of Bis(1-methylindenyl)chromium(II), $(Ind^{Me-1})_2Cr$. $CrCl_2$ (0.100 g, 0.814 mmol) and $Li[Ind^{Me-1}]$ (0.222 g, 1.63 mmol) were placed in a flask equipped with a magnetic stirring bar. Approximately 40 mL of THF was added, which immediately produced a dark purple solution. The mixture was stirred overnight, after which the solvent was removed under vacuum to leave a purple solid. Hexanes (20 mL) was added, and all insoluble impurities were removed by filtration over a medium-porosity frit. The filtrate was collected in a small Schlenk flask and was capped and placed in a freezer. After 8 h, small green crystals of $(Ind^{Me-1})_2Cr$ had formed; once no additional crystal growth was observed, the filtrate was separated from the solid by cannulation on a Schlenk line. The crystals were dried under vacuum and taken into a glovebox for further characterization. The remaining filtrate was stripped to dryness to afford additional solid (total yield: 0.192 g, 76%), mp 123 °C. Anal. Calcd for $C_{20}H_{18}Cr$: C, 77.40; H, 5.85; Cr, 16.75. Found: C, 77.48; H, 5.96; Cr, 16.33. Principal IR bands (cm^{-1}): 2960 (m), 2928 (m), 2866 (w), 1260 (w), 1082 (s), 1005 (s), 611 (s). Solution magnetic susceptibility ($\mu_{eff}^{T(K)}$, ±0.2 μ_B): $4.69^{182.8}$, $4.74,^{193}$ $4.77,^{203}$ $4.79^{213.2}$, $4.78^{223.2}$, $4.83^{233.1}$, $4.83^{242.6}$, $4.81^{251.4}$, $4.81^{263.1}$, $4.76^{272.8}$, 4.75^{283}, 4.73^{298}.

Synthesis of Bis(2-methylindenyl)chromium(II), $(Ind^{Me-2})_2Cr$. $CrCl_2$ (0.365 g, 2.97 mmol) and $K[Ind^{Me-2}]$ (1.00 g, 5.94 mmol) were placed in a 125 mL Erlenmeyer flask equipped with a magnetic stirring bar. Approximately 30 mL of THF was added, which immediately produced a dark green solution. The mixture was stirred overnight, during which time the solution turned a deep purple. The solvent was then removed under vacuum to leave a dark purple solid. Approximately 40 mL of hexanes was added, and all insoluble impurities were removed by filtration over a medium-porosity frit. An additional 100 mL of hexanes was added because of the limited solubility of the product. The filtrate was collected in a 250 mL Schlenk flask, which was capped with a rubber septum and placed in a −30 °C freezer. After 16 h, small purple crystals of $(Ind^{Me-2})_2Cr$ were observed. The mother liquor was separated from the crystalline solid by cannulation on a Schlenk line. The crystals were dried under vacuum and taken into a glovebox for isolation (0.445 g, 48% yield), mp 160−162 °C. Anal. Calcd for $C_{20}H_{18}Cr$: C, 77.40; H, 5.85; Cr, 16.75. Found: C, 77.48; H, 5.59; Cr, 17.15. Solution magnetic susceptibility ($\mu_{eff}^{T(K)}$, ±0.2 μ_B): 4.8^{240}, 4.8^{250}, 4.7^{270}, 4.5^{300}.

Attempted Synthesis of Bis(4-methylindenyl)chromium(II), $(Ind^{Me-4})_2Cr$. Anhydrous $CrCl_2$ (0.0828 g, 0.674 mmol) was added to a 125 mL Erlenmeyer flask along with a magnetic stirring bar and 10 mL of THF. $K[Ind^{Me-4}]$ (0.189 g, 1.35 mmol) was dissolved

(12) Overby, J. S.; Hanusa, T. P.; Sellers, S. P.; Yee, G. T. *Organometallics* **1999**, *18*, 3561−3562.
(13) Crisp, J. A.; Meredith, M. B.; Hanusa, T. P.; Wang, G.; Brennessel, W. W.; Yee, G. T. *Inorg. Chem.* **2005**, *44*, 172−174.
(14) Williams, R. A.; Tesh, K. F.; Hanusa, T. P. *J. Am. Chem. Soc.* **1991**, *113*, 4843−4851.
(15) (a) Evans, D. F. *J. Chem. Soc*. **1959**, 2003−2005. (b) Loeliger, J.; Scheffold, R. *J. Chem. Educ*. **1972**, *49*, 646−647. (c) Grant, D. H. J. *Chem. Educ*. **1995**, 72, 39−40. (d) Sur, S. K. *J. Magn. Reson*. **1989**, *82*, 169−173.
(16) Hays, M. L. Ph.D. Thesis, Vanderbilt University, 1996.
(17) Kobayashi, T.; Tanaka, K.; Miwa, J.; Katsumura, S. *Tetrahedron: Asymmetry* **2004**, *15*, 185−188.
(18) Cedheim, L.; Eberson, L. *Synthesis* **1973**, 159.
(19) Perrin, D. D.; Armarego, W. L. F. *Purification of Laboratory Chemicals*, 3rd ed.; Pergamon: Oxford, 1988.

Table 1. Crystal Data and Summary of X-ray Data Collection

	$(Ind^{Me-1})_2Cr$ (105 K)	$(Ind^{Me-1})_2Cr$ (173 K)	$(Ind^{Me-1})_2Cr$ (298 K)	$(Ind^{Me-2})_2Cr$ (173 K)	$(Ind^{Me-4})(\mu\text{-}Ind^{Me-4})\text{-}Cr_2(\mu\text{-}Cl)\cdot 0.5(toluene)$
formula	$C_{20}H_{18}Cr$	$C_{20}H_{18}Cr$	$C_{20}H_{18}Cr$	$C_{20}H_{18}Cr$	$C_{30}H_{27}ClCr_2\cdot 0.50(C_7H_8)$
fw	310.34	310.34	310.34	310.34	573.02
color of cryst	green	green	green	purple	brown
cryst dimens, mm	0.40 × 0.40 × 0.25	0.40 × 0.18 × 0.18	0.40 × 0.40 × 0.25	0.16 × 0.08 × 0.06	0.05 × 0.05 × 0.33
space group	$P2_1/c$	$P2_1/c$	$P2_1/c$	$P2_1/c$	$P2_1/c$
cell dimens					
a, Å	12.266(3)	12.3215(12)	12.438(4)	8.703(3)	24.675(4)
b, Å	9.718(2)	9.7409(9)	9.792(3)	7.814(2)	6.7882(10)
c, Å	12.391(3)	12.5025(12)	12.739(4)	11.732(4)	16.172(2)
β, deg	96.560(4)	97.049(2)	96.179(5)	99.357(6)	95.473(2)
volume, Å^3	1467.4(6)	1489.2(2)	1542.6(7)	787.2(4)	2696.5(7)
Z	4	4	4	2	4
calcd density, Mg/m^3	1.405	1.384	1.336	1.309	1.412
abs coeff, mm^{-1}	0.769	0.758	0.732	0.717	0.926
F(000)	648	648	648	324	1188
radiation type	Mo Kα (0.71073 Å)	Mo Kα (0.71073 Å)	Mo Kα (0.71073 Å)	Mo Kα (0.71073 Å)	Mo Kα (0.71073 Å)
temperature, K	105(2)	173(2)	298(1)	173(2)	173(2)
limits of data collection	$1.67° < \theta < 27.96°$	$1.67° < \theta < 25.04°$	$1.65° < \theta < 25.03°$	$2.37° < \theta < 25.02°$	$0.83° \le \theta \le 25.05°$
index ranges	$-16 < h < 16$, $0 < k < 12$, $0 < l < 16$	$-14 < h < 14$, $-11 < k < 11$, $-14 < l < 14$	$-14 < h < 14$, $0 < k < 11$, $0 < l < 15$	$-10 < h < 10$, $-9 < k < 9$, $-13 < l < 12$	$-29 \le h \le 29$, $-8 < k \le 6$, $-19 \le l \le 19$
total no. of reflcns collected	17 270	10 677	11 384	3740	15 782
no. of unique reflcns	3486 ($R_{int} = 0.0331$)	2635 ($R_{int} = 0.035$)	2715 ($R_{int} = 0.0229$)	1378 ($R_{int} = 0.060$)	4718 ($R_{int} = 0.0921$)
transmn factors	0.7484−0.8310	0.7514−0.8757	0.7585−0.8383	0.8939−0.9583	0.7686−0.9552
no. of data/restraints/param	3486/0/192	2635/0/190	2715/0/192	1378/0/98	4718/169/367
R indices ($I > 2\sigma(I)$)	$R = 0.0477$, $R_w = 0.1240$	$R = 0.0378$, $R_w = 0.0932$	$R = 0.0475$, $R_w = 0.1324$	$R = 0.0491$, $R_w = 0.1128$	$R = 0.0849$, $R_w = 0.1924$
R indices (all data)	$R = 0.0609$, $R_w = 0.1341$	$R = 0.0471$, $R_w = 0.1024$	$R = 0.0587$, $R_w = 0.1432$	$R = 0.0792$, $R_w = 0.1296$	$R = 0.1619$, $R_w = 0.2190$
goodness of fit on *F*2	1.078	1.048	1.063	1.052	1.043
max./min. peak in final diff map, e$^-$/Å^3	1.780/−0.608	0.713/−0.675	1.060/−0.257	0.395/−0.459	0.684/−0.425

in 10 mL of THF and added dropwise to the flask while stirring. The mixture initially turned brown, then black, and it was allowed to stir 8 h before removing the solvent under vacuum. Toluene (10 mL) was added to dissolve the chromium complex, and the mixture was filtered through a medium-porosity glass frit. Removal of the THF left $(Ind^{Me-4})_3Cr_2Cl$ as a dark brown solid (0.274 g, 72%). Diffusion of hexanes into a toluene solution of the complex lead to the formation of dark brown crystals within 1 day. The crystals were unstable at room temperature and turned green within 2 days.

Computational Details. Density functional theory calculations were performed using the Gaussian 03W suite of programs.[20] The fractional coordinates from single X-ray crystal determinations were used to define the molecular structures. The BP86 functional was used, which incorporates Becke's exchange functional[21] with the 1986 gradient-corrected correlation functional of Perdew.[22] The standard 6-31G(d) basis set was used on all atoms. Frontier orbitals were visualized with GaussView 3.

General Procedures for X-ray Crystallography. Suitable crystals of $(Ind^{Me-1})_2Cr$, $(Ind^{Me-2})_2Cr$, and $(Ind^{Me-4})_3Cr_2Cl$ were located, attached to glass fibers, and mounted on a Siemens smart system for data collection at various temperatures. Data collection and structure solutions for all molecules were conducted at the X-ray Crystallography Laboratory at the University of Minnesota. The intensity data were corrected for absorption (SADABS). All calculations were performed with the SHELXTL suite of programs.[23] Final cell constants were calculated from a set of strong reflections measured during the actual data collection. Relevant crystal and data collection parameters for each of the compounds are given in Table 1.

The space groups were determined from systematic absences and intensity statistics. A direct-methods solution was calculated that provided most of the non-hydrogen atoms from the E-maps. Several full-matrix least squares/difference Fourier cycles were performed that located the remainder of the non-hydrogen atoms. All non-hydrogen atoms were refined with anisotropic displacement parameters. All hydrogen atoms were placed in ideal positions and refined as riding atoms with relative isotropic displacement parameters.

X-ray Crystallography of $(Ind^{Me-2})_2Cr$. Deep purple crystals of $(Ind^{Me-2})_2Cr$ were isolated from a concentrated hexanes solution that was cooled to −30 °C. The crystals were separated from the mother liquor via cannulation and dried under vacuum prior to data collection at 173 K. The metal lies on an inversion center in space group $P2_1/c$, rendering only one-half of the molecule unique.

X-ray Crystallography of $(Ind^{Me-1})_2Cr$. Dark green crystals of $(Ind^{Me-1})_2Cr$ were isolated from concentrated hexanes or THF/toluene solutions. Data collection was repeated at temperatures of 105, 173, and 298 K.

(20) Frisch, M. J.; Trucks, G. W.; Schlegel, H. B.; Scuseria, G. E.; Robb, M. A.; Cheeseman, J. R.; Montgomery, J. A., Jr.; Vreven, T.; Kudin, K. N.; Burant, J. C.; Millam, J. M.; Iyengar, S. S.; Tomasi, J.; Barone, V.; Mennucci, B.; Cossi, M.; Scalmani, G.; Rega, N.; Petersson, G. A.; Nakatsuji, H.; Hada, M.; Ehara, M.; Toyota, K.; Fukuda, R.; Hasegawa, J.; Ishida, M.; Nakajima, T.; Honda, Y.; Kitao, O.; Nakai, H.; Klene, M.; Li, X.; Knox, J. E.; Hratchian, H. P.; Cross, J. B.; Bakken, V.; Adamo, C.; Jaramillo, J.; Gomperts, R.; Stratmann, R. E.; Yazyev, O.; Austin, A. J.; Cammi, R.; Pomelli, C.; Ochterski, J. W.; Ayala, P. Y.; Morokuma, K.; Voth, G. A.; Salvador, P.; Dannenberg, J. J.; Zakrzewski, V. G.; Dapprich, S.; Daniels, A. D.; Strain, M. C.; Farkas, O.; Malick, D. K.; Rabuck, A. D.; Raghavachari, K.; Foresman, J. B.; Ortiz, J. V.; Cui, Q.; Baboul, A. G.; Clifford, S.; Cioslowski, J.; Stefanov, B. B.; Liu, G.; Liashenko, A.; Piskorz, P.; Komaromi, I.; Martin, R. L.; Fox, D. J.; Keith, T.; Al-Laham, M. A.; Peng, C. Y.; Nanayakkara, A.; Challacombe, M.; Gill, P. M. W.; Johnson, B.; Chen, W.; Wong, M. W.; Gonzalez, C.; Pople, J. A. *Gaussian 03*, Revision C.02; Gaussian, Inc.: Wallingford, CT, 2004.

(21) Becke, A. D. *Phys. Rev. A* **1988**, *38*, 3098−3100.

(22) Perdew, J. P. *Phys. Rev. B* **1986**, *33*, 8822−8824.

(23) *SHELXTL*, 6.1 ed.; Bruker Analytical X-Ray Systems: Madison, WI, 2000.

X-ray Crystallography of $(Ind^{Me-4})_3Cr_2Cl$. Dark brown needles of $(Ind^{Me-4})_3Cr_2Cl$ were isolated from concentrated toluene upon slow diffusion of hexanes into the solution at room temperature. One-half of a toluene molecule per dichromium unit was also detected in the lattice. More details are provided in the Supporting Information.

Results and Discussion

Ligand Synthesis. All three methylindenes (1-, 2-, and 4-) are readily deprotonated by *n*-BuLi in hexanes (eq 1) or $K[N(SiMe_3)_2]$ in toluene (eq 2). The transmetallating agent potassium *tert*-butoxide was successfully used with the corresponding lithium indenides, affording the potassium analogues as powders. Although $HInd^{Me-4}$ is miscible in toluene at all concentrations, $K[Ind^{Me-4}]$ is sparingly soluble in toluene and precipitates from the reaction mixture as a bright yellow powder; the other indenides are white to off-white. The indenides are generally formed in high yield and are easily purified by filtration followed by several washings with hexanes. They are air- and moisture-sensitive and must be stored under an inert atmosphere to prevent decomposition.

$$HInd^{Me-(1\text{ or }2)} + n\text{-BuLi} \xrightarrow[-n\text{-butane}]{\text{hexane}} Li[Ind^{Me-(1\text{ or }2)}] \quad (1)$$

$$HInd^{Me-(2\text{ or }4)} + K[N(SiMe_3)_2] \xrightarrow[-HN(SiMe_3)_2]{\text{toluene}} K[Ind^{Me-(2\text{ or }4)}] \quad (2)$$

Synthesis of Substituted Bis(indenyl)chromium(II) Complexes. Bis(indenyl)chromium(II) complexes were readily synthesized from the 1- and 2-methylindenide salts by metathesis/halide elimination reactions. Two equivalents of the appropriate indenide salt were allowed to react with anhydrous chromium(II) chloride in THF (eq 3). The solutions were stirred overnight (>16 h) to ensure complete reaction.

$$2\ M[Ind^{Me-x}] + CrCl_2 \xrightarrow{THF} (Ind^{Me-x})_2Cr + 2\ MCl \quad (3)$$

$$M = Li;\ x = 1 \text{ or } 2;\ M = K;\ x = 2$$

The purified bis(indenyl)chromium(II) complexes were crystallized either by slow evaporation of solvent from a saturated solution or by cooling of a concentrated solution to approximately −30 °C. The $(Ind^{Me-1})_2Cr$ and $(Ind^{Me-2})_2Cr$ complexes are indefinitely stable at room temperature under a nitrogen atmosphere.

In contrast, under similar conditions the 2:1 reaction of $CrCl_2$ with $K[Ind^{Me-4}]$ does not produce $(Ind^{Me-4})_2Cr$, either as a monomer or as a dimeric $[(Ind^{Me-4})_2Cr]_2$ complex (as observed for the unsubstituted indenyl ligand, i.e., $[Ind_2Cr]_2$ [11]). Instead, the chloride-bridged complex $(Ind^{Me-4})_3Cr_2Cl$ is isolated; crystals of it can be grown by diffusion of hexane into a toluene solution of the complex. It is much less thermally stable than the mononuclear bis(indenyl) species and decomposes within 2 days at room temperature in the solid state. To prevent deterioration, it must be handled and stored below −20 °C.

It is worth noting that when equal molar amounts of $CrCl_2$ and sodium indenide react, the chloride-bridged dimer Ind_3Cr_2Cl is isolated.[11] Subsequent treatment with a second equivalent of sodium indenide leads to the bis(indenyl)chromium(II) dimer, $[Ind_2Cr]_2$. The isolation of the chloride derivative is solely a function of the starting ratios of reagents, as a 2:1 reaction of sodium indenide with $CrCl_2$ produces $[Ind_2Cr]_2$ directly. In this regard, the change produced by a single methyl group on the benzo portion of the indenyl ligand is striking. It is possible that the formation of $[(Ind^{Me-4})_2Cr]_2$ is slow and that $(Ind^{Me-4})_3Cr_2Cl$ represents an unstable kinetic product. If so, more forcing reaction conditions might drive the reaction to form $(Ind^{Me-4})_2Cr$ eventually.

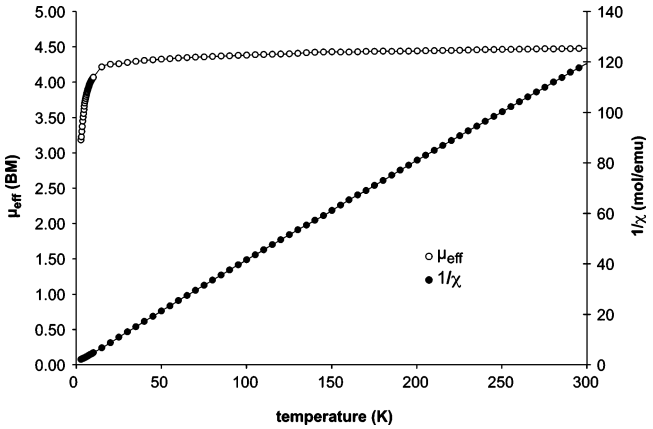

Figure 1. SQUID data for $(Ind^{Me-2})_2Cr$. Effective magnetic moment (BM) and $1/\chi$ (mol/emu) plotted as a function of temperature.

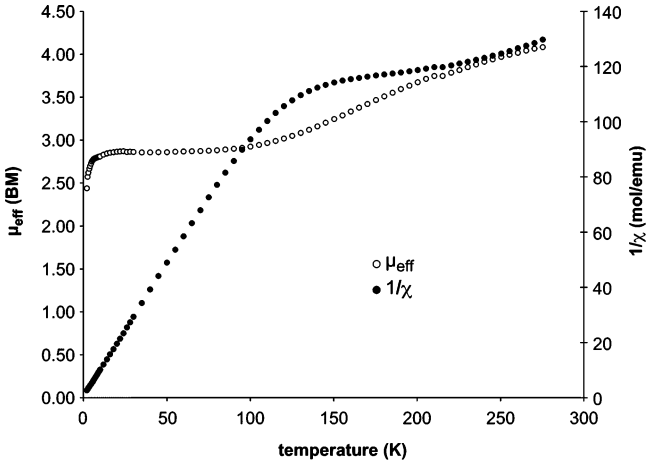

Figure 2. SQUID data for $(Ind^{Me-1})_2Cr$. Effective magnetic moment (BM) and $1/\chi$ (mol/emu) plotted as a function of temperature.

Solid State Magnetic Susceptibility Measurements. Crystalline samples of $(Ind^{Me-1})_2Cr$ and $(Ind^{Me-2})_2Cr$ were examined with a SQUID magnetometer, and Figures 1 and 2 show $1/\chi$ and effective magnetic moment (μ_{eff}) as a function of temperature for both compounds.

$(Ind^{Me-2})_2Cr$. The magnetic moment measured for $(Ind^{Me-2})_2Cr$ indicates that it is a high-spin complex down to 25 K in the solid state; there is some zero-field splitting exhibited by the complex below 25 K (Figure 1). Above 25 K, the effective magnetic moment (4.3−4.4 μ_B) is lower than the spin-only value for four unpaired electrons (4.9 μ_B), but it is consistent with the moments observed for other high-spin complexes of this type.[10,12] $(Ind^{Me-2})_2Cr$ exhibits simple Curie law behavior from 25 to 300 K; the plot of $1/\chi$ versus T intersects the origin.

$(Ind^{Me-1})_2Cr$ displays Curie law behavior below 75 K; a small amount of zero-field splitting is found below 20 K. The complex is low-spin ($S = 1$) with a moment (2.87 μ_B) close to the spin-only value for two unpaired electrons ($\mu_B = 2.83$). Above 75 K, the complex begins to undergo spin-crossover, and the effective magnetic moment reaches 4.1 μ_B by 275 K. This value is somewhat less than the expected spin-only value

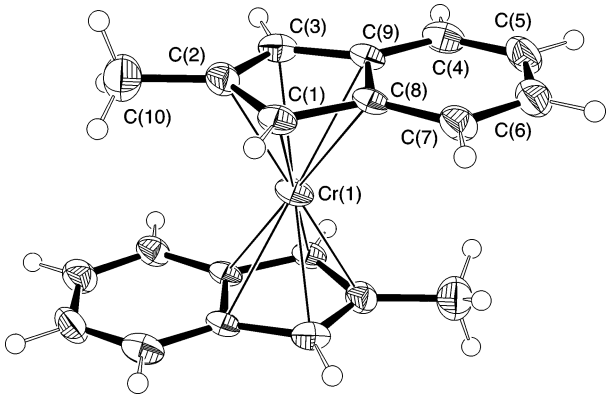

Figure 3. ORTEP of $(Ind^{Me-2})_2Cr$, illustrating the numbering scheme used in the text. Thermal ellipsoids are shown at the 50% level.

Table 2. Selected Bond Distances (Å) and Angles (deg) for $(Ind^{Me-2})_2Cr$

atoms	distance	atoms	angle
Cr(1)−C(1)	2.243(3)	inter-C_5 ring plane angle	0.0
Cr(1)−C(2)	2.253(3)	hinge angle[a]	6.9
Cr(1)−C(3)	2.255(3)	fold angle[a]	1.6
Cr(1)−C(8)	2.394(3)		
Cr(1)−C(9)	2.393(3)		

[a] For definitions of these angles, see ref 32.

for a high-spin bis(indenyl) chromium species (cf. $\mu_B = 4.5\ \mu_B$ at 275 K in the high-spin $(Ind^{2i})_2Cr$), suggesting an incomplete transition.[12]

Solution NMR Magnetic Susceptibility Measurements of Bis(indenyl)chromium(II) Complexes. Variable-temperature magnetic susceptibility studies (Evans' method[15,24]) indicate that $(Ind^{Me-2})_2Cr$ has a $\mu_{eff} > 4.5\ \mu_B$ from 240 to 300 K, which is consistent with four unpaired electrons. $(Ind^{Me-1})_2Cr$ was also found to be a high-spin species in solution, displaying $\mu_{eff} > 4.6\ \mu_B$ from 183 to 298 K; note that over a similar range in the solid state (185−275 K), μ_{eff} varies from 3.55 to 4.08 μ_B. Although green in the solid state, the complex is purple in solution, a color found with other substituted high-spin complexes of its type.

Solid State Structures. $(Ind^{Me-2})_2Cr$. Crystals of $(Ind^{Me-2})_2Cr$ were isolated from cold hexanes as purple blocks. Only one-half of the molecule is unique, as the chromium lies on an inversion center. An ORTEP of the molecule is given in Figure 3, which indicates the numbering scheme referred to in the text; selected bond lengths and angles are provided in Table 2. The average Cr−C ring distance of 2.308(7) Å is similar to that in high-spin bis(indenyl)chromium(II) complexes, which have average Cr−C ring distances near 2.3 Å.[10,12] The ligands are bound in an η^5 fashion to the chromium and are staggered 180° with respect to each another. The bridgehead C−Cr contacts (av 2.394 Å) are longer than the C−Cr distances of C(1) and C(3) (av 2.249 Å). The range of Cr−C bonds ($\Delta_{M-C} = 0.145$ Å) is similar to values found in other high-spin $(indenyl')_2Cr$-(II) compounds and does not represent slippage to an η^3-binding mode.[25] Little distortion is present within the indenyl ligands; for example, the methyl substituent is displaced out of the five-membered-ring plane away from the metal by 0.093 Å, corresponding to an angle of 1.5°.

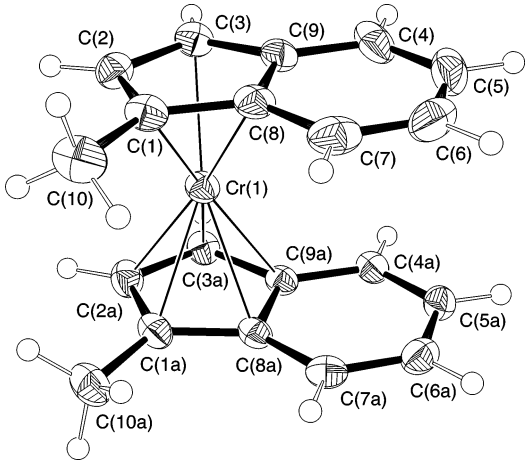

Figure 4. ORTEP of $(Ind^{Me-1})_2Cr$ at 105 K, illustrating the numbering scheme used in the text. Thermal ellipsoids are shown at the 50% level.

Table 3. Selected Bond Distances (Å) and Angles (deg) for $(Ind^{Me-1})_2Cr$ (105 K)

atoms	distance	atoms	distance
Cr(1)−C(1)	2.160(3)	Cr(1)−C(1a)	2.176(3)
Cr(1)−C(2)	2.127(3)	Cr(1)−C(2a)	2.129(3)
Cr(1)−C(3)	2.143(3)	Cr(1)−C(3a)	2.139(3)
Cr(1)−C(8)	2.230(3)	Cr(1)−C(8a)	2.237(2)
Cr(1)−C(9)	2.226(3)	Cr(1)−C(9a)	2.220(2)
C_5 ring planes	6.8		
hinge angle[a]	2.2 (av)		
fold angle[a]	3.7 (av)		
twist[a]	2.4		

[a] For definitions of these angles, see ref 32.

Table 4. Selected Bond Distances (Å) and Angles (deg) for $(Ind^{Me-1})_2Cr$ (173 K)

atoms	distance	atoms	angle
Cr(1)−C(1)	2.182(2)	Cr(1)−C(1a)	2.196(2)
Cr(1)−C(2)	2.144(3)	Cr(1)−C(2a)	2.149(3)
Cr(1)−C(3)	2.161(3)	Cr(1)−C(3a)	2.159(2)
Cr(1)−C(8)	2.269(2)	Cr(1)−C(8a)	2.271(2)
Cr(1)−C(9)	2.264(2)	Cr(1)−C(9a)	2.259(2)
C_5 ring planes	5.5		
hinge angle[a]	3.0 (av)		
fold angle[a]	3.0 (av)		
twist[a]	2.5		

[a] For definitions of these angles, see ref 32.

$(Ind^{Me-1})_2Cr$. Crystals of $(Ind^{Me-1})_2Cr$ were obtained as green blocks and examined at 105, 173, and 298 K. The structure of the molecule as determined from data obtained at 105 K is discussed first; an ORTEP of the complex is given as Figure 4, which indicates the numbering scheme referred to in the text. Drawings for the molecules obtained at other temperatures are available in the Supporting Information. Selected bond lengths and angles of the structures at all three temperatures are given in Tables 3−5.

105 K Data. The two indenyl ligands flank the chromium center in an eclipsed *meso* configuration, with an angle of 7° between the C_5 rings. The Cr−C ring distances (av 2.179(9) Å) are consistent with a low-spin chromium(II) center; low-spin species in this series display average Cr−C bond distances between 2.18 and 2.22 Å.[10,26] Both rings are bound in an η^5 fashion to the chromium; the range of Cr−C bonds ($\Delta_{M-C} = 0.074$ Å) is similar to values observed in other substituted Ind'_2-

(24) Lindoy, L. F.; Katovic, V.; Busch, D. H. *J. Chem. Educ.* **1972**, *49*, 117−120.

(25) Faller, J. W.; Crabtree, R. H.; Habib, A. *Organometallics* **1985**, *4*, 929−935.

(26) O'Hare, D.; Murphy, V. J.; Kaltsoyannis, N. *J. Chem. Soc., Dalton Trans.* **1993**, 383−392.

Table 5. Selected Bond Distances (Å) and Angles (Deg) for $(Ind^{Me-1})_2Cr$ (298 K)

atoms	distance	atoms	distance
Cr(1)−C(1)	2.226(3)	Cr(1)−C(1a)	2.236(3)
Cr(1)−C(2)	2.190(4)	Cr(1)−C(2a)	2.199(4)
Cr(1)−C(3)	2.202(3)	Cr(1)−C(3a)	2.200(3)
Cr(1)−C(8)	2.344(3)	Cr(1)−C(8a)	2.351(3)
Cr(1)−C(9)	2.337(3)	Cr(1)−C(9a)	2.338(3)
C_5 ring planes	1.3		
hinge angle[a]	5.5 (av)		
fold angle[a]	1.0 (av)		
twist[a]	2.5		

[a] For definitions of these angles, see ref 32.

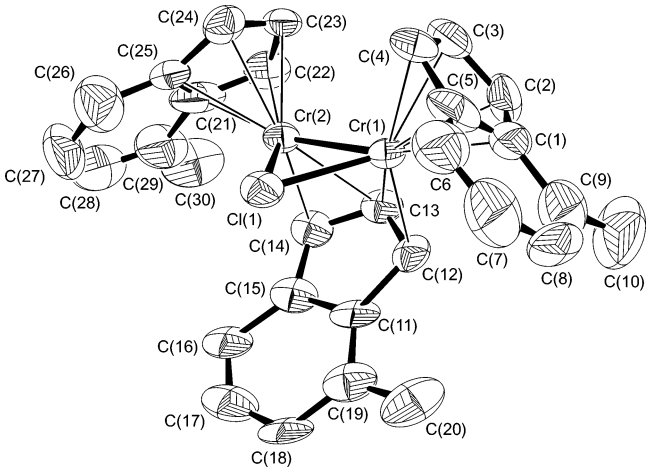

Figure 5. ORTEP of the non-hydrogen atoms of $(Ind^{Me-4})_3Cr_2Cl$ at 173 K, illustrating the numbering scheme used in the text. Thermal ellipsoids are shown at the 50% level.

Cr complexes. The methyl groups are only slightly displaced from the C_5 planes (av out-of-plane bending angle away from the metal of 1.9°).

173 K Data. The Cr−C ring distances (av 2.205(7) Å) have lengthened by 0.026 Å compared to the structure at 105 K, but are still representative of a low-spin Cr(II) species. The spread in Cr−C distances ($\Delta_{M-C} = 0.091$ Å) is slightly larger than at 105 K. The rings remain slightly canted, with an angle of 5.5° between the two five-membered-ring planes. Relative to the C_5 rings, the methyl substituents display an average out-of-plane bending angle away from the metal of 1.2°.

298 K Data. The average Cr−C ring distance (2.262(10) Å) is 0.083 Å longer that at 105 K, a 3.8% change. Although ring slippage is more pronounced at the higher temperature ($\Delta_{M-C} = 0.127$ Å), the canting between the two ring planes (1.3°) is less than at lower temperatures. The methyl groups display an average out-of-plane bending angle away from the metal of 1.1°.

$(Ind^{Me-4})_3Cr_2Cl$. Crystals of $(Ind^{Me-4})_3Cr_2Cl$ were obtained as dark brown needles and examined at 173 K. An ORTEP of the complex is given as Figure 5, which indicates the numbering scheme referred to in the text. Disorder in the indenyl ligands lowers the accuracy of the structure, but it is clear that the compound is isostructural with Ind_3Cr_2Cl.[11] The Cr−Cr bond distance of 2.325(2) Å is slightly longer than that found for the nonmethylated compound (2.317(1) Å). There are two terminal η^5-indenyl ligands, each one bound to a separate metal center. The molecule is completed by a μ,η^3-indenyl ligand and a bridging chloride. The three indenyl ligands form a tripod-like arrangement around the two Cr centers, but are splayed out to accommodate the μ-Cl ligand. This arrangement leads to two of the methyl groups pointing toward each other, although the closest intramolecular Me···Me′ contacts are at 4.5 Å, outside the sum of van der Waals radii.

Table 6. Allowed Overlap of Metal d Orbitals with Indenyl π Orbitals of Various Symmetries

C_{2h}	d orbital overlap	C_{2v}	d orbital overlap	C_2	d orbital overlap
A_g	x^2, y^2, z^2, xy	A_1	x^2, y^2, z^2	A	x^2, y^2, z^2, xy
B_g	yz, xz	A_2	xy	B	xz, yz
A_u		B_1	xz		
B_u		B_2	yz		

Structural and Magnetic Difference between $(Ind^{Me-2})_2Cr$ and $(Ind^{Me-1})_2Cr$. Introduction of a single methyl group to the five-membered ring of the indenyl ligand produces monomeric species. The methyl substituent evidently interferes with existence of the metal−metal bond between the two chromium centers, so that analogues to the known dimeric $[Ind_2Cr]_2$ complex are not isolated. The magnetically simpler species is $(Ind^{Me-2})_2Cr$, which is high-spin (four unpaired electrons) in both solution and the solid state over a wide temperature range. This is consistent with the conclusion that a staggered, centrosymmetric structure supports the high spin state in substituted Ind'_2Cr complexes.[10]

In contrast, $(Ind^{Me-1})_2Cr$ is found with ligands in an eclipsed *meso* conformation. Eclipsed rings are sometimes found in methylated metallocene analogues, a few of which include $(CpMe)_2Cr$,[27] $(CpMe)_2Fe$,[28] and $(1,3\text{-}Me_2C_5H_3)_2Ru$.[29] It has been suggested that packing forces dictate the conformation of the cyclopentadienyl rings in these species, and it is possible that the same effect is operative in $(Ind^{Me-1})_2Cr$. The spin crossover behavior observed in $(Ind^{Me-1})_2Cr$ can be correlated to structural changes in the species with temperature change. At 105 K in the solid state, the complex is in the low-spin form; above this temperature, the structure begins to exhibit crossover behavior and is near a high spin state at 275 K. Over this temperature range, the average M−C bond distances lengthen linearly by 4.3×10^{-4} Å K^{-1}. It should be noted that $(Ind^{Me-1})_2Cr$ is a strictly high-spin species in solution from 182 to 298 K. Once the complex is dissolved, the ligands evidently can rotate freely; they likely adopt a predominantly staggered conformation.

Orbital Interactions in Ind_2Cr. The interaction of transition metal d orbitals with the π orbitals of the indenyl anion has been described for staggered (with C_{2h} or C_i symmetry),[10,30] eclipsed (ideally C_{2v}-symmetric),[31] and gauche (ideally C_2-symmetric, but in known examples effectively C_1)[10] conformations. In the first case, which is applicable to $(Ind^{Me-2})_2Cr$, the A_u and B_u symmetric combinations of the indenyl π orbitals cannot interact with the d orbitals. These restrictions are relaxed under C_{2v} or lower symmetry (Table 6). Note also that, although of little energetic importance, combinations of indenyl π orbitals with effective σ and δ bonding symmetry would not display similar symmetry effects. Single-point DFT calculations performed on the solid state structure data were used to generate frontier orbital images that illustrate the effect of the symmetry

(27) Benetollo, F.; Camporese, A.; Rossetto, G. *Acta Crystallogr., Sect. C* **1994**, *C50*, 1002−1003.
(28) Foucher, D. A.; Honeyman, C. H.; Lough, A. J.; Manners, I.; Nelson, J. M. *Acta Crystallogr., Sect. C* **1995**, *51*, 1795−1799.
(29) Kirss, R. U.; Quazi, A.; Lake, C. H.; Churchill, M. R. *Organometallics* **1993**, *12*, 4145−4150.
(30) O'Hare, D.; Green, J. C.; Marder, T.; Collins, S.; Stringer, G.; Kakkar, A. K.; Kaltsoyannis, N.; Kuhn, A.; Lewis, R.; Mehnert, C.; Scott, P.; Kurmooo, M.; Pugh, S. *Organometallics* **1992**, *11*, 48−55.
(31) Crossley, N. S.; Green, J. C.; Nagy, A.; Stringer, G. *J. Chem. Soc., Dalton Trans.* **1989**, 2139−2147.
(32) Trnka, T. M.; Bonanno, J. B.; Bridgewater, B. M.; Parkin, G. *Organometallics* **2001**, *20*, 3255−3264.

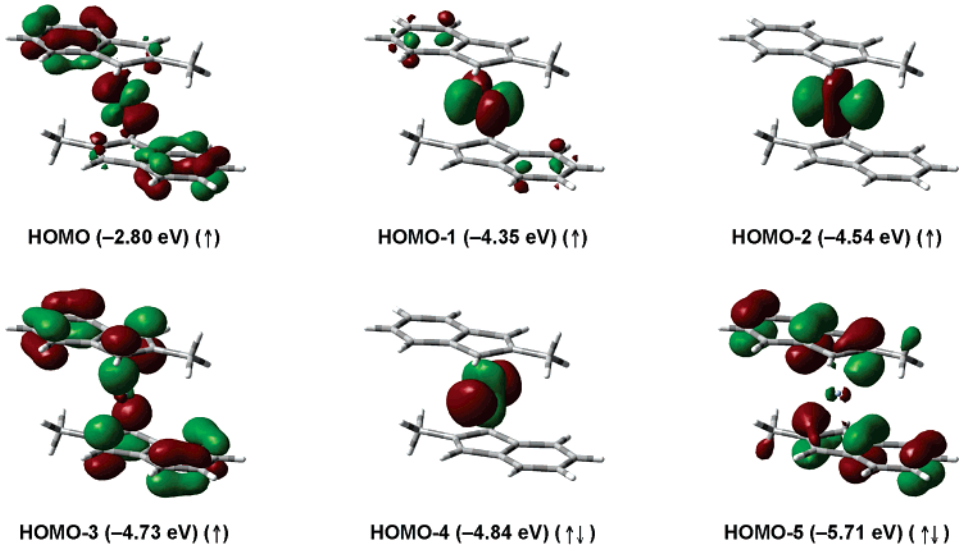

Figure 6. Frontier orbitals of $(Ind^{Me-2})_2Cr$ (HOMO to HOMO−5). All isodensity values are 0.040 au.

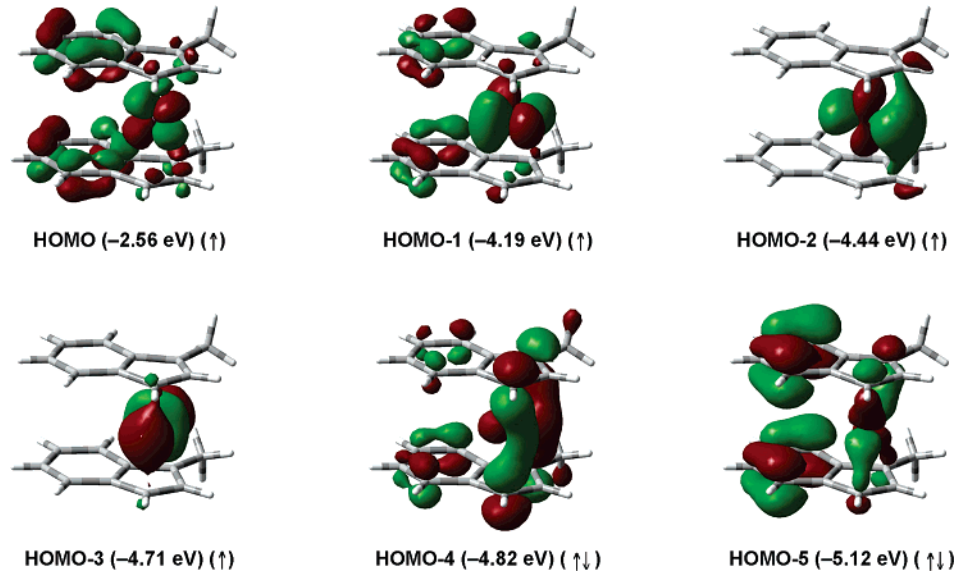

Figure 7. Frontier orbitals of $(Ind^{Me-1})_2Cr$ (298 K) (HOMO to HOMO−5). All isodensity values are 0.040 au.

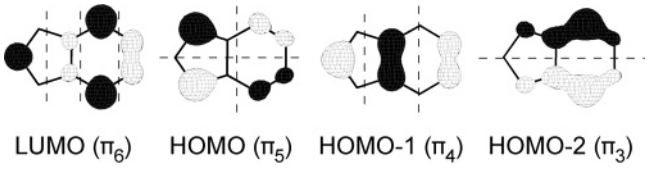

Figure 8. Frontier π orbitals of the indenyl anion. The π_n notation is the same as that used by previous authors (ref 43).

restrictions (Figures 6 and 7). Although the location of the methyl groups determines the relative orientation of the indenyl ligands in the complexes, they appear to have little effect on the interaction of the metal with the indenyl π orbitals. For the staggered $(Ind^{Me-2})_2Cr$ and the eclipsed $(Ind^{Me-1})_2Cr$ (298 K structure), the four highest energy orbitals were set as singly occupied, in accordance with the magnetic data. The HOMO for each complex is composed of an antibonding combination of the d_{xz} orbitals and π_4 (HOMO−1) of the indenyl anion (Figure 8). For $(Ind^{Me-2})_2Cr$, the HOMO−1 to HOMO−5 orbitals are effectively nonbonding. In the case of HOMO−3 and HOMO−5, which are ligand π orbitals of A_u and B_u symmetry, respectively, the lack of interaction with the metal is enforced by symmetry restrictions.

Generally greater d−ligand π mixing is observed in the frontier orbitals of $(Ind^{Me-1})_2Cr$ (Figure 7); in HOMO−4, the d_{xy} and the π_5 combinations of the ligand π orbitals, and in HOMO−5 the d_{xz} and π_5 interactions, are appreciable. A DFT calculation based on the 105 K structural data (not shown) indicates that the extent of mixing increases on cooling, so that the antibonding d_{xz}/π_4 combination is raised substantially above the energy of the $d_{x^2-y^2}$ orbital, which has now become the HOMO. The changes in energy levels are evidenced by the differences in the HOMO−LUMO gap, i.e., $(Ind^{Me-2})_2Cr$ (1.09 eV) < $(Ind^{Me-1})_2Cr$ (1.22 eV at 298 K) < $(Ind^{Me-1})_2Cr$ (1.70 eV at 105 K). The increase in the HOMO−LUMO gap leads to an increase in spin pairing and a low-spin complex at 105 K.

Conclusions

The dimerization observed in bis(indenyl)chromium(II) is prevented by the addition of a single methyl substituent to the five-membered ring. Addition of a methyl group to the benzo portion of the indenyl ligand may not be as effective in this regard, perhaps because it need not directly interfere with the Cr···Cr′ metal bonding. The particular conformations (eclipsed

and staggered) adopted by $(Ind^{Me-1})_2Cr$ and $(Ind^{Me-2})_2Cr$ in the solid state are not readily rationalizable, and there does not appear to be any reason either could not adopt that of the other. The magnetic evidence that both are probably in the staggered conformation in solution suggests that the eclipsed conformation of $(Ind^{Me-1})_2Cr$ is imposed by crystal packing forces.

The identification of the spin-crossover behavior in solid $(Ind^{Me-1})_2Cr$ expands the range of magnetic behavior known for bis(indenyl)chromium complexes. Symmetry constraints are operative in eclipsed $(Ind^{Me-1})_2Cr$, but not to the same extent in the staggered $(Ind^{Me-2})_2Cr$. In the latter, no interaction is allowed between the A_u and B_u combinations of the π orbitals of the indenyl anion and the metal d orbitals, ensuring that their electrons remain nonbonding in the complex. Under the idealized C_{2v} symmetry of the eclipsed $(Ind^{Me-1})_2Cr$, specific metal d−ligand π orbital matching is required, but no sets of π orbitals are excluded from interaction. The greater interaction between the ligand and metal orbitals evidently helps make the complex more responsive to temperature changes, so that contraction on cooling increases the orbital mixing and the HOMO−LUMO gap, ultimately leading to the low spin state. The previously described[10] gauche complexes take this a step further and relax the symmetry constraints so that extensive mixing of the metal and ligand-based orbitals is possible; this has been identified as the origin of the gauche complexes' permanently low spin state.

It has been shown that electron-donating substituents can also affect the spin state of a bis(indenyl)chromium compound; for example, the permethylated complex $(C_9Me_7)_2Cr$ is low-spin, despite its staggered geometry.[26] This suggests that the combination of symmetry restrictions and site-specific multiple ligand substitution could lead to more varied magnetic behavior in bis(indenyl)metal complexes, a possibility we are investigating.

Acknowledgment. We thank the Petroleum Research Fund, administered by the American Chemical Society, for support of this research and the NSF for partial funding of the SQUID magnetometer. E.D.B. was supported with a GAANN Fellowship from the Department of Education. Guangbin Wang is thanked for help with magnetic measurements, and a reviewer is thanked for helpful comments.

Supporting Information Available: The X-ray crystallographic files in CIF format for $(Ind^{Me-2})_2Cr$, $(Ind^{Me-1})_2Cr$ (105, 173, and 298 K), and $(Ind^{Me-4})_3Cr_2Cl$. ORTEPs are also given for $(Ind^{Me-1})_2Cr$ at 173 and 298 K. These are available free of charge via the Internet at http://pubs.acs.org.

OM060534U